

Electronic supplementary information (ESI)

Multiple photosynthetic reaction centres of porphyrinic polypeptide-Li⁺@C₆₀ supramolecular complexes

Kei Ohkubo,^{*ab} Tetsuya Hasegawa,^a Régis Rein,^c Nathalie Solladié^{*c} and Shunichi Fukuzumi^{*abd}

^a Department of Material and Life Science, Graduate School of Engineering, Osaka University, ALCA and SENTAN, Japan Science and Technology Agency (JST), Suita, Osaka 565-0871, Japan. E-mail: fukuzumi@chem.eng.osaka-u.ac.jp; Fax: +81-6-6879-7370

^b Department of Chemistry and Nano Science, Ewha Womans University, Seoul 120-750, Korea.

^d Groupe de Synthèse de Systèmes Porphyriniques (G2SP), Laboratoire de Chimie de Coordination du CNRS, BP 44099 205 route de Narbonne 31077 Toulouse Cedex 4, France

^e Faculty of Science and Technology, Meijo University, ALCA and SENTAN, Japan Science and Technology Agency (JST), Nagoya, Aichi 468-8502, Japan

Experimental details

Materials. General chemicals of the best grade available were purchased from commercial suppliers and were used without further purification. Unless otherwise noted, benzonitrile (PhCN) was distilled over two times phosphorus pentoxide (P_2O_5), and potassium carbonate (K_2CO_3) before use. Lithium-ion-encapsulated fullerene hexafluorophosphate salt ($Li^+@C_{60} PF_6^-$, Idea International Corporation) was commercially obtained from Wako Pure Chemical Industries, Ltd., Japan.

Spectral measurements. Absorption spectra were recorded on a JASCO V-670 spectrophotometer at room temperature. Phosphorescence spectra were measured on a Horiba FluoroMax-4 spectrofluorophotometer. A 2-methyltetrahydrofuran (2-MeTHF)/ethyl iodide (EtI) (9:1) solution of porphyrin $P(H_2P)_1$ in a quartz tube (3 mm in diameter) were degassed by nitrogen bubbling for 10 min prior to the measurements. The sample tube was put in a quartz liquid nitrogen Dewar flask. The measurements were carried out by excitation at 425 nm. Fluorescence spectra were recorded on a Horiba FluoroMax-4 spectrofluorophotometer. The measurements were carried out by excitation at 425 nm. in deaerated PhCN. The solution was degassed by nitrogen bubbling for 10 min prior to the measurements.

Electrochemical measurements. Differential pulses voltammetry (DPV) studies were carried out using an ALS-630B electrochemical analyzer in deaerated PhCN or in a mixed solvent (DMSO and PhCN) containing 0.1 M TBAPF₆ as a supporting electrolyte at 298 K. A conventional three-electrode cell was used with a carbon working electrode (surface area = 0.3 mm²) and a platinum wire as the counter electrode. The carbon working electrode, purchased from BAS, was routinely polished with a polishing alumina suspension from BAS and rinsed with distilled water and acetonitrile before use. The potentials were measured with respect to an Ag/AgNO₃ (10 mM) reference electrode. All electrochemical measurements were carried out under a nitrogen atmosphere. The values of redox potentials (*vs.* Ag/AgNO₃) are converted into those *vs.* SCE by addition of 0.29 V.¹

Laser flash photolysis measurements. Nanosecond transient absorption spectral measurements were made according to the following procedure. A deaerated solutions containing $Li^+@C_{60}$ with anionic phthalocyanines were excited by a Panther OPO pumped Nd: YAG laser (Continuum, SLII-10, 4-6 ns fwhm) at 355 nm. The resulting time resolved transient absorption spectra were measured by using a continuous Xe-lamp (150 W) and a photodiode (Hamamatsu 2949) as the probe light and detector, respectively. The output from the photodiode and the photomultiplier tube was recorded

using a digitizing oscilloscope (Tektronix, TDS3032, 300 MHz). The solutions were deoxygenated by N₂ purging for 10 min prior to measurements. Rates of photoinduced electron-transfer reactions were monitored by the rise and decay of the absorption band due to the Li⁺@C₆₀ radical anion. First-order rate constants were determined by a least-squares curve fit. All experiments were performed at 298 K.

Femtosecond transient absorption spectroscopy experiments were conducted using an ultrafast source: Integra-C (Quantronix Corp.), an optical parametric amplifier: TOPAS (Light Conversion Ltd.) and a commercially available optical detection system: Helios provided by Ultrafast Systems LLC. The source for the pump and probe pulses were derived from the fundamental output of Integra-C (780 nm, 2 mJ/pulse and fwhm = 130 fs) at a repetition rate of 1 kHz. 75% of the fundamental output of the laser was introduced into TOPAS which has optical frequency mixers resulting in tunable range from 285 nm to 1660 nm, while the rest of the output was used for white light generation. Prior to generating the probe continuum, a variable neutral density filter was inserted in the path in order to generate stable continuum, then the laser pulse was fed to a delay line that provides an experimental time window of 3.2 ns with a maximum step resolution of 7 fs. In our experiments, a wavelength at 425 nm of TOPAS output, which is fourth harmonic of signal or idler pulses, was chosen as the pump beam. As this TOPAS output consists of not only desirable wavelength but also unnecessary wavelengths, the latter was deviated using a wedge prism with wedge angle of 18°. The desirable beam was irradiated at the sample cell with a spot size of 1 mm diameter where it was merged with the white probe pulse in a close angle (< 10°). The probe beam after passing through the 2 mm sample cell was focused on a fibre optic cable that was connected to a CCD spectrograph for recording the time-resolved spectra (410-800 nm). Typically, 2500 excitation pulses were averaged for 5 seconds to obtain the transient spectrum at a set delay time. Kinetic traces at appropriate wavelengths were assembled from the time-resolved spectral data. All measurements were conducted at room temperature, 295 K.

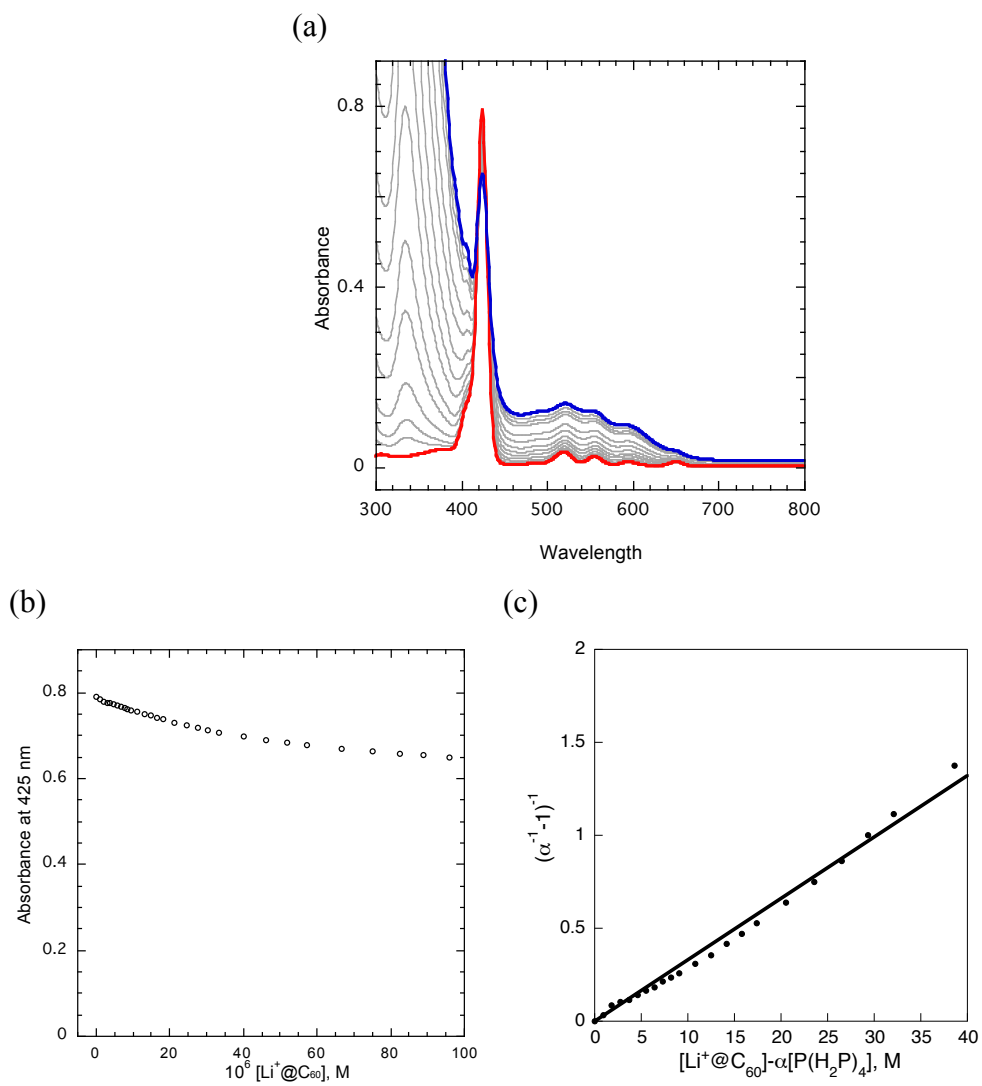
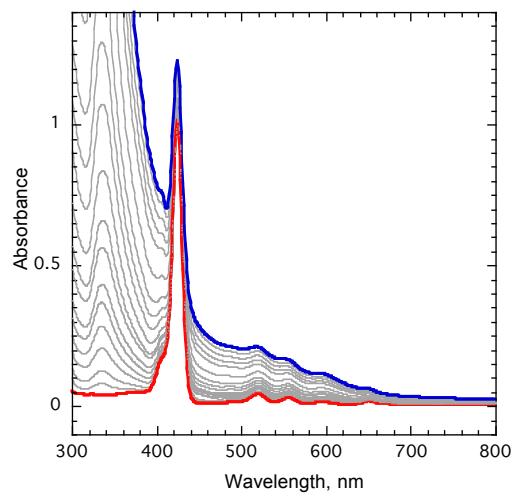


Fig. S1 (a) UV-vis absorption spectra of $P(H_2P)_4$ in the presence of various concentrations of $Li^+@C_{60}$ (0 – 96 μM) in PhCN at 298 K; (b) Absorption profile at 425 nm. (c) Benesi-Hildebrand plot for determination of association constant.

(a)



(b)

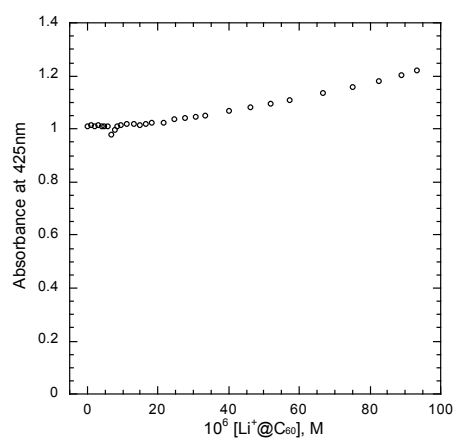


Fig. S2 (a) UV-vis absorption spectra of P(H₂P)₂ in the presence of various concentrations of Li⁺@C₆₀ (0 – 96 μM) in PhCN at 298 K; (b) Absorption profile at 425 nm.

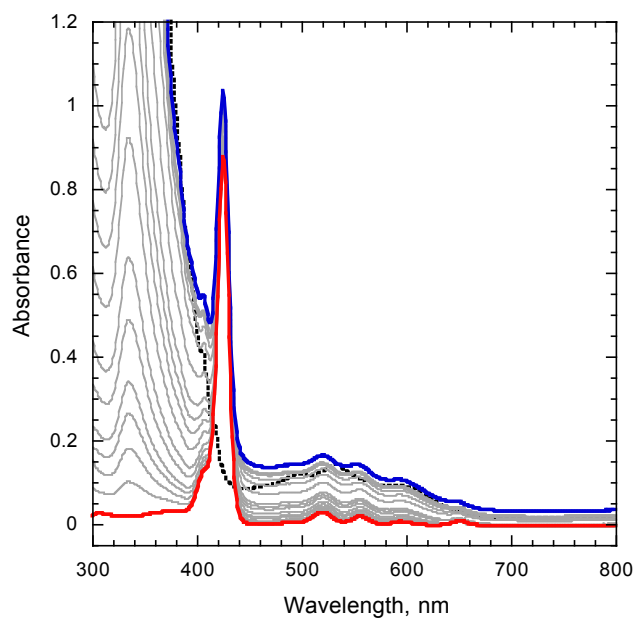


Fig. S3 UV-vis absorption spectra of $\text{P}(\text{H}_2\text{P})_1$ in the presence of various concentrations of $\text{Li}^+@C_{60}$ (0 – 96 μM) in PhCN at 298 K.

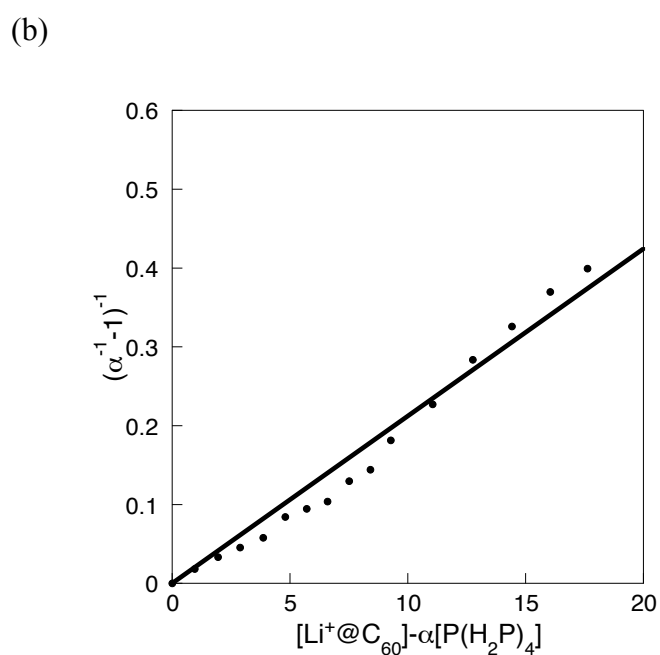
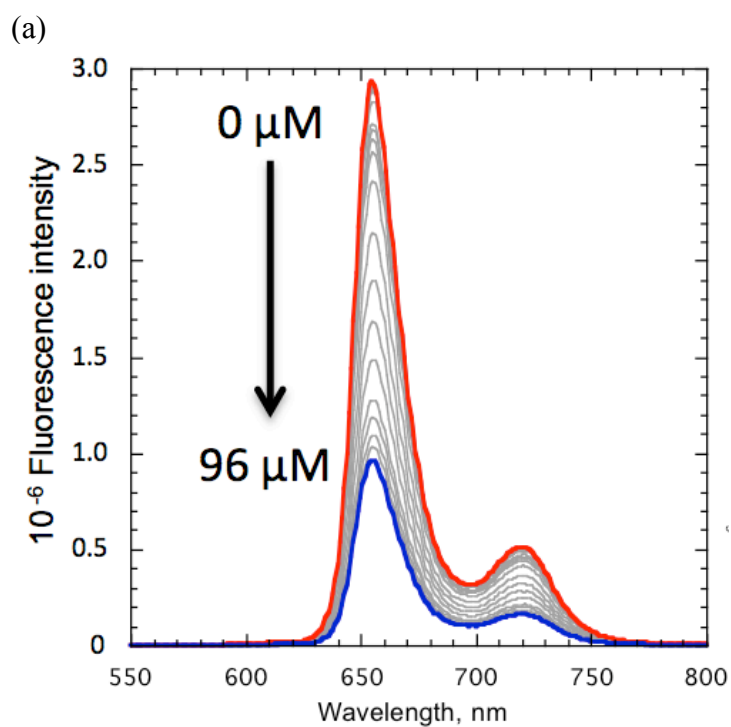


Fig. S4 (a) Fluorescence spectra of $\text{P}(\text{H}_2\text{P})_4$ in the presence of various concentrations of $\text{Li}^+\text{@C}_{60}$ in PhCN at 298 K; (b) Benesi-Hildebrand plot for determination of association constant.

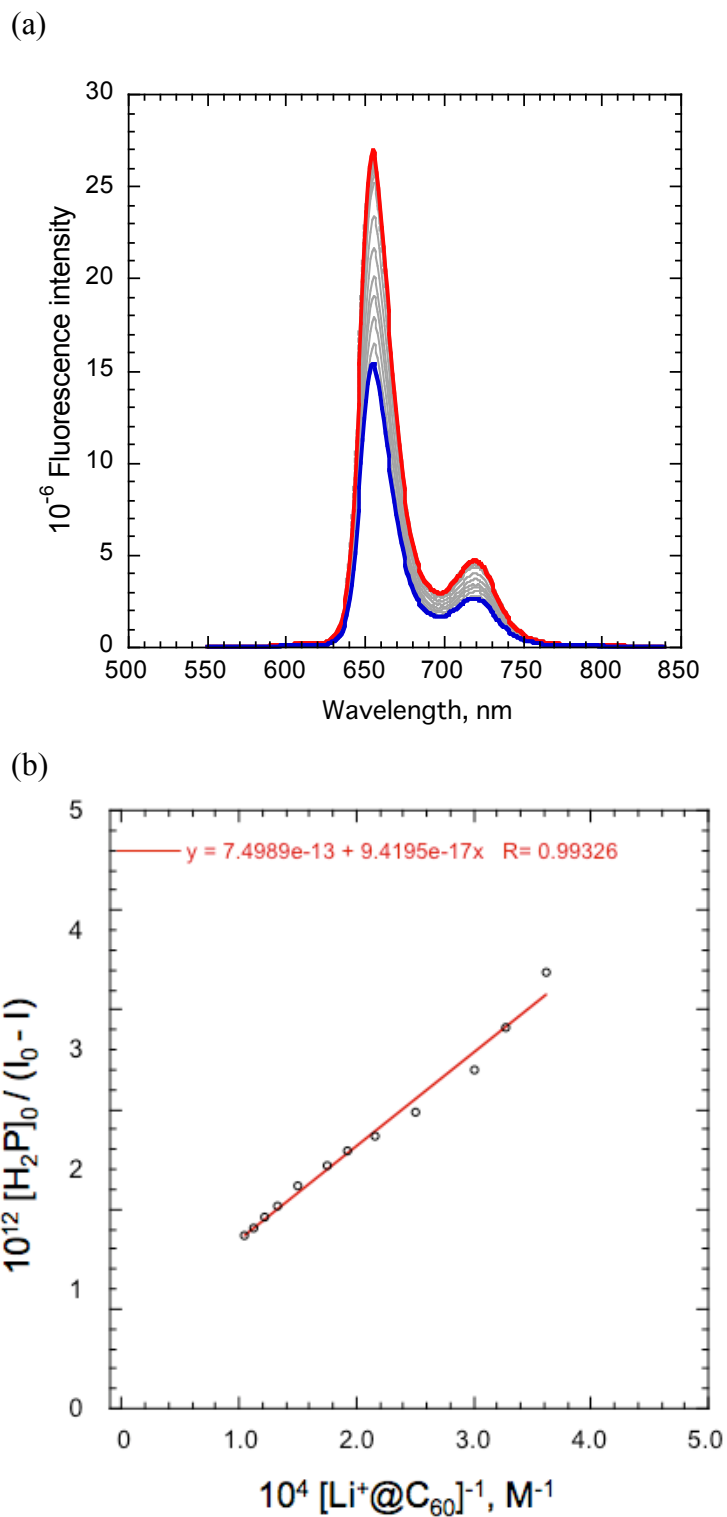


Fig. S5 (a) Fluorescence spectra of $\text{P}(\text{H}_2\text{P})_2$ in the presence of various concentrations of $\text{Li}^+\text{@C}_{60}$ in PhCN at 298 K; (b) Benesi-Hildebrand plot for determination of association constant.

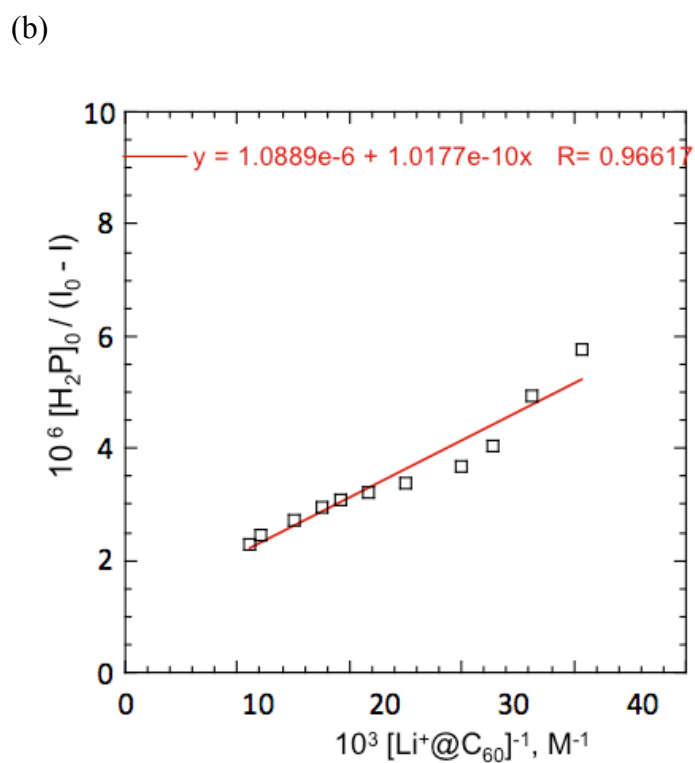
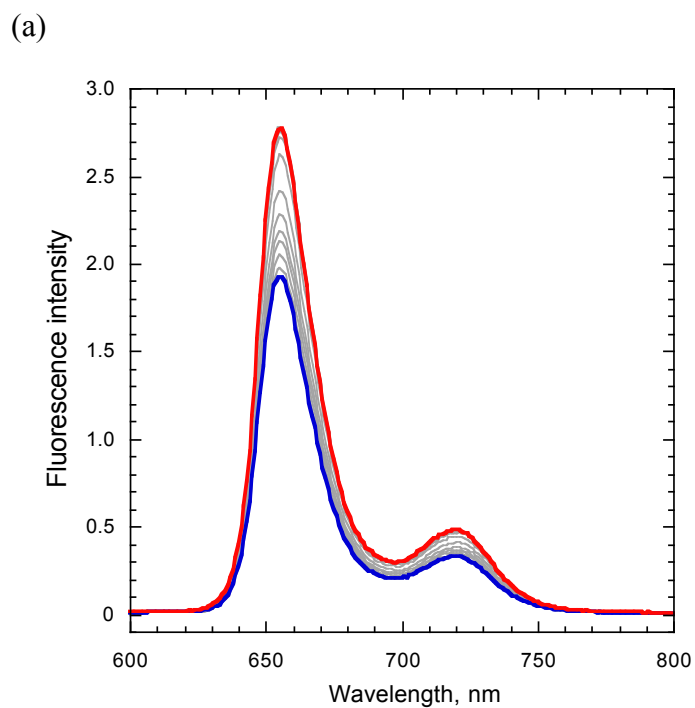


Fig. S6 (a) Fluorescence spectra of $P(H_2P)_1$ in the presence of various concentrations of $Li^+@C_{60}$ in PhCN at 298 K; (b) Benesi-Hildebrand plot for determination of association constant.

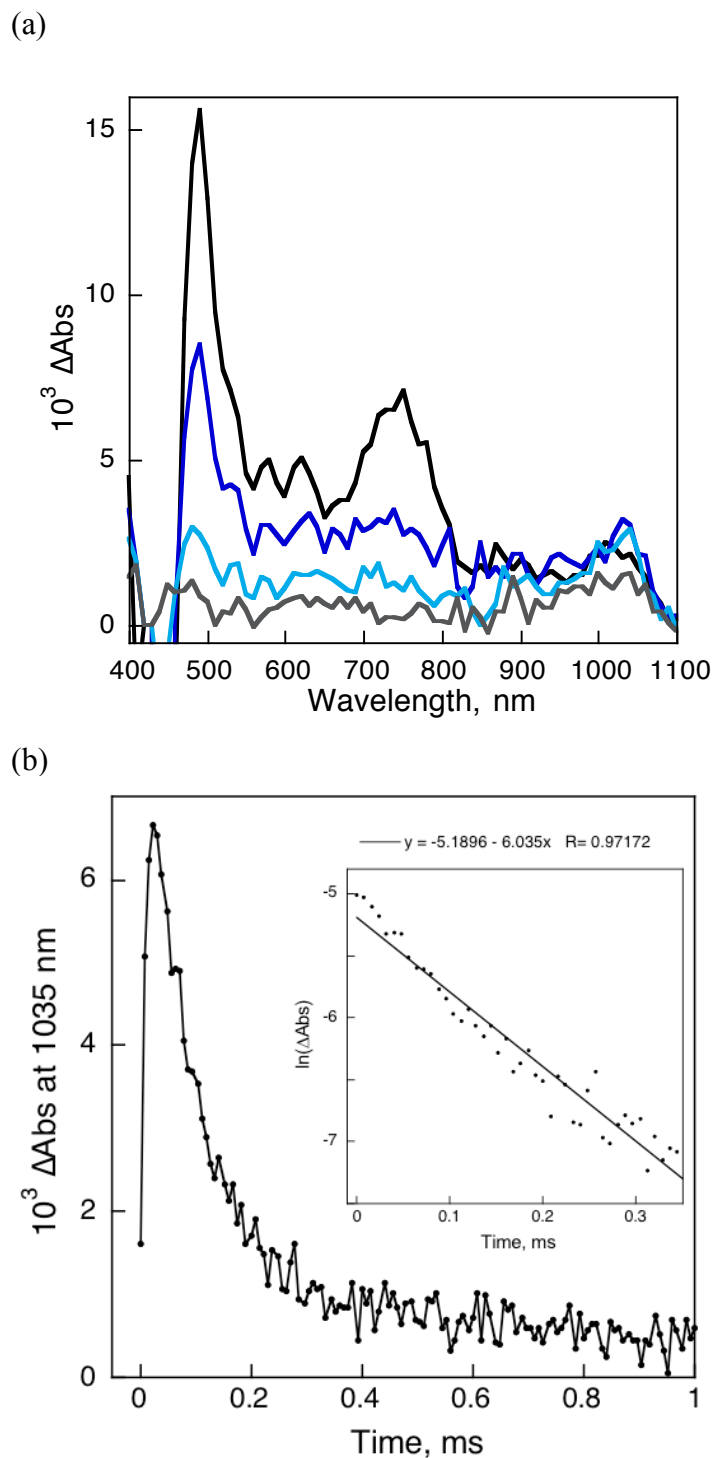


Fig. S7 Transient absorption spectra of $\text{P}(\text{H}_2\text{P})_4$ (5.2×10^{-6} M) with $\text{Li}^+@\text{C}_{60}$ (4.0×10^{-5} M) in deaerated PhCN observed after nanosecond laser flash excitation taken at 8 (black), 32 (blue) and 96 (sky blue) and 200 μs (gray). Excitation wavelength: 532 nm. (b) Decay time profile at 1035 nm with the different laser pulse intensities (2 - 5 mJ pulse $^{-1}$).

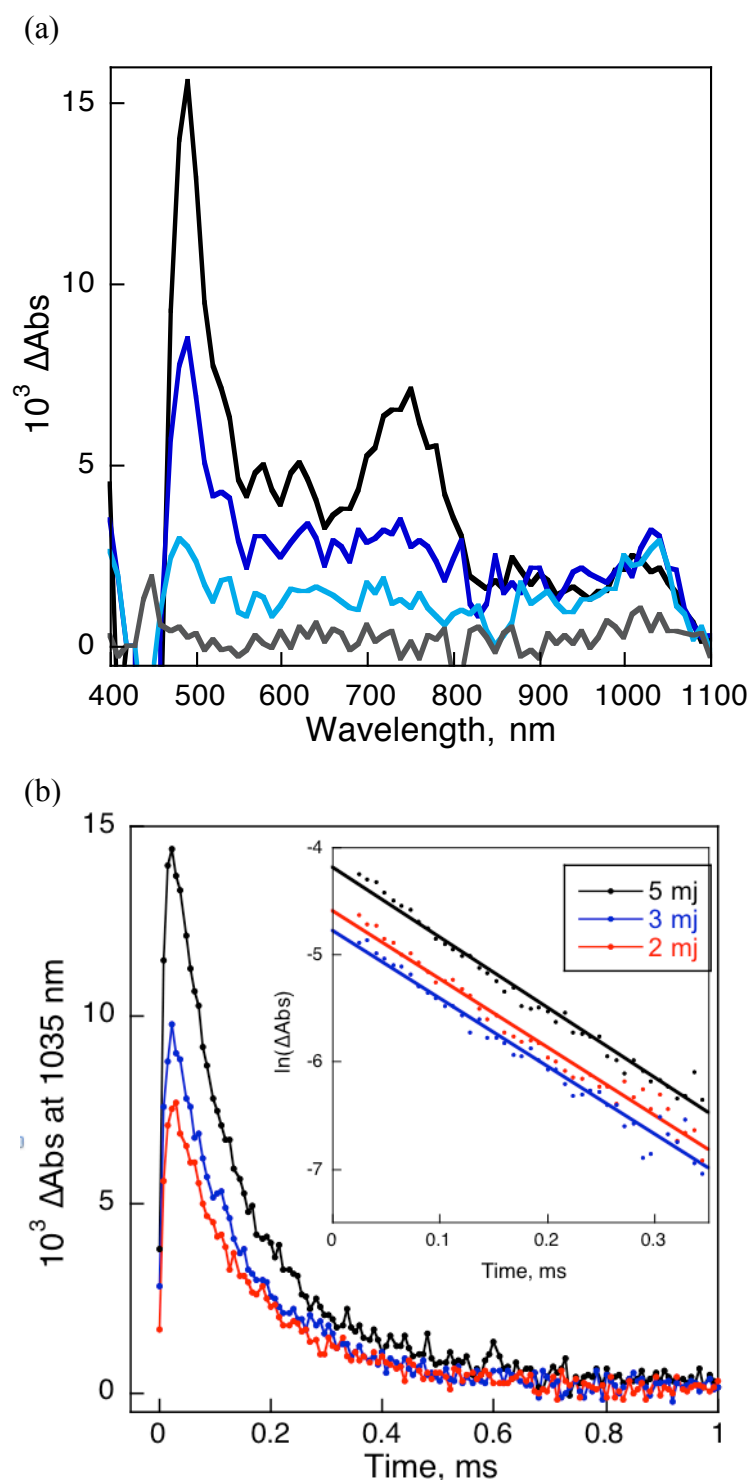


Fig. S8 Transient absorption spectra of $\text{P}(\text{H}_2\text{P})_2$ (1.0×10^{-5} M) with $\text{Li}^+@\text{C}_{60}$ (4.0×10^{-5} M) in deaerated PhCN observed after nanosecond laser flash excitation taken at 8 (black), 32 (blue) and 96 (sky blue) and 200 μs (gray). Excitation wavelength: 532 nm. (b) Decay time profile at 1035 nm with the different laser pulse intensities (2 - 5 mJ pulse⁻¹).

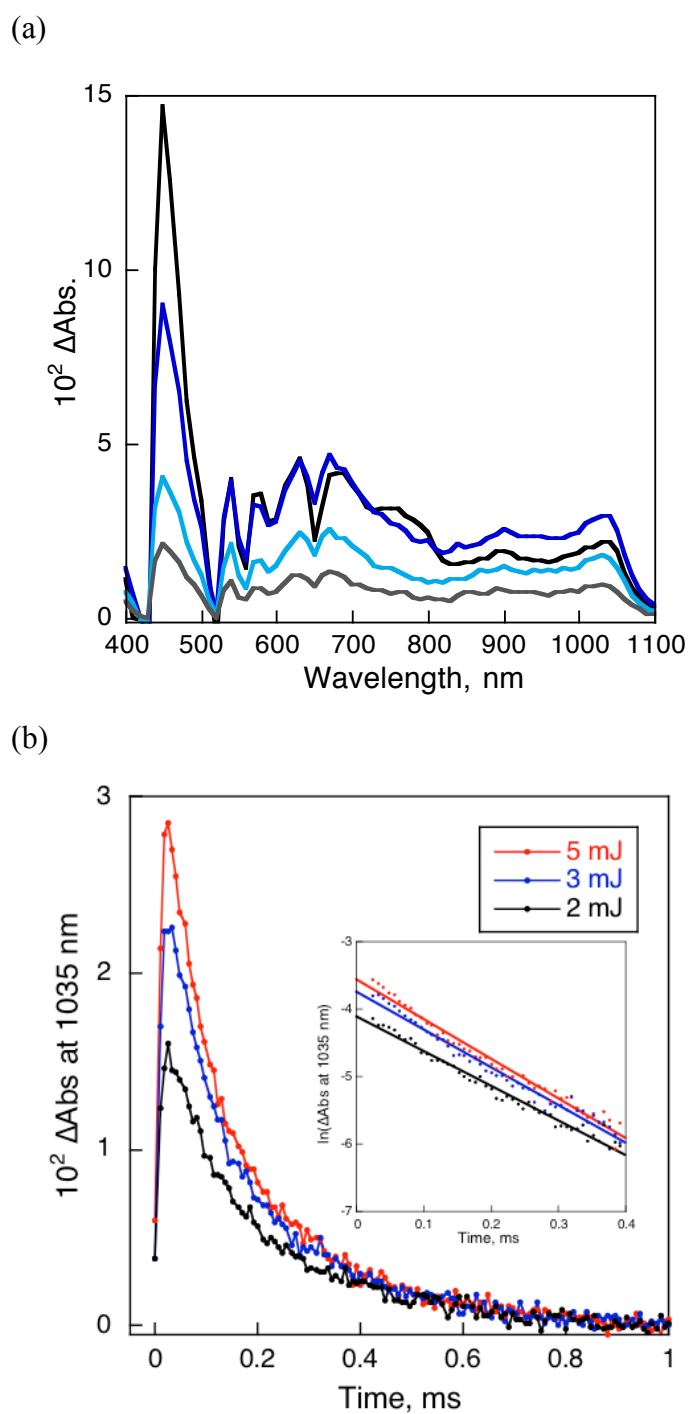


Fig. S9 Transient absorption spectra of $\text{P}(\text{H}_2\text{P})_1$ (2.0×10^{-5} M) with $\text{Li}^+@\text{C}_{60}$ (4.0×10^{-5} M) in deaerated PhCN observed after nanosecond laser flash excitation taken at 8 (black), 32 (blue) and 96 (sky blue) and 200 μs (gray). Excitation wavelength: 532 nm. (b) Decay time profile at 1035 nm with the different laser pulse intensities (2 - 5 mJ pulse⁻¹).

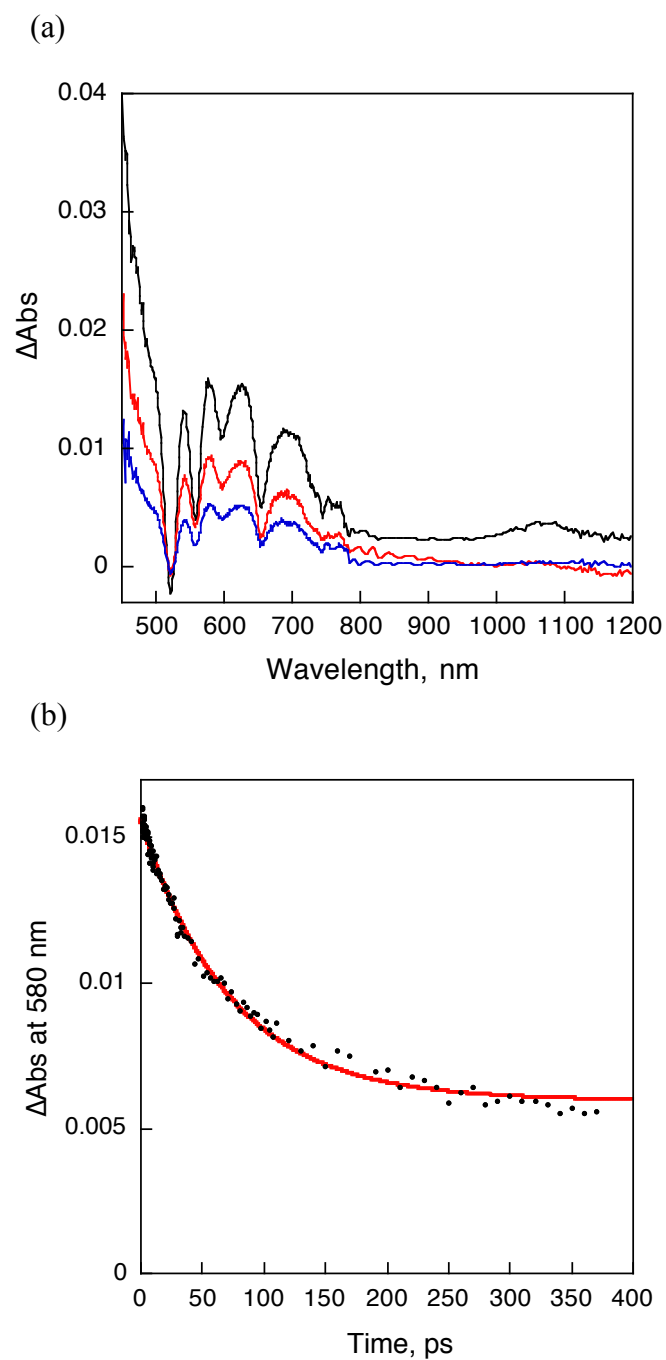


Fig. S10 (a) Transient absorption spectra of $P(H_2P)_8$ (5.2×10^{-6} M) in deaerated PhCN observed after femtosecond laser flash excitation. Excitation wavelength: 425 nm. (b) Decay time profile at 580 nm with a three-exponential decay curve fitting.

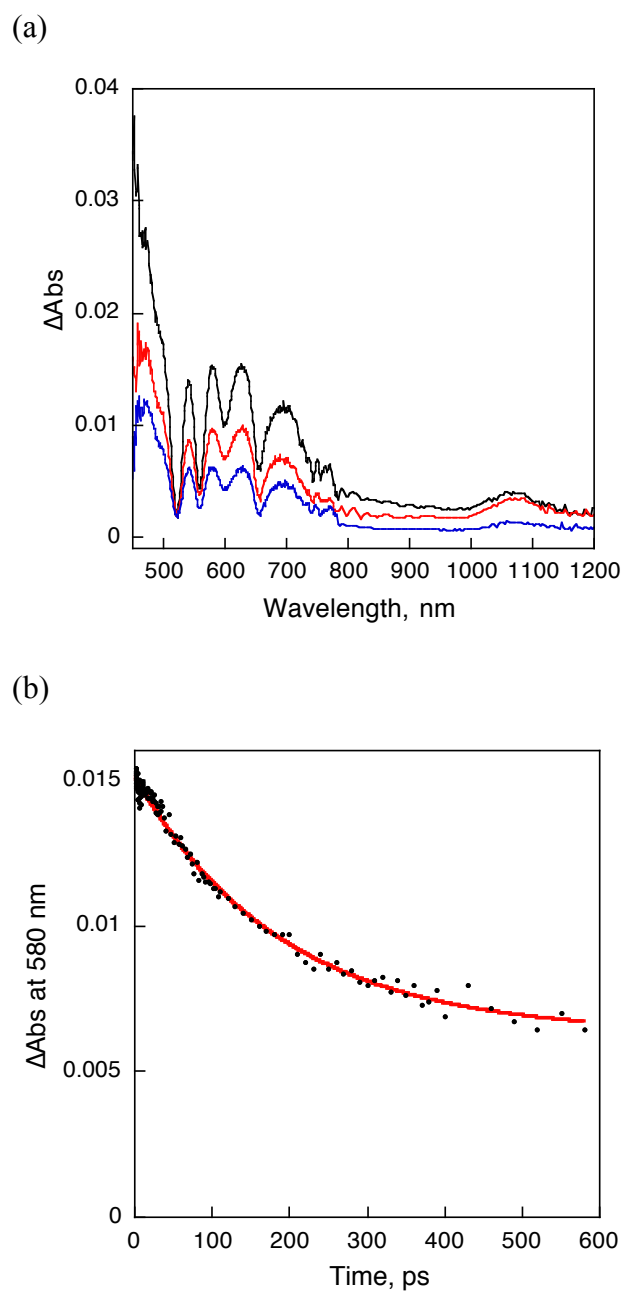


Fig. S11 (a) Transient absorption spectra of $\text{P}(\text{H}_2\text{P})_4$ (1.3×10^{-6} M) with $\text{Li}^+@\text{C}_{60}$ (2.0×10^{-5} M) in deaerated PhCN observed after femtosecond laser flash excitation. Excitation wavelength: 425 nm. (b) Decay time profile at 580 nm with a three-exponential decay curve fitting..

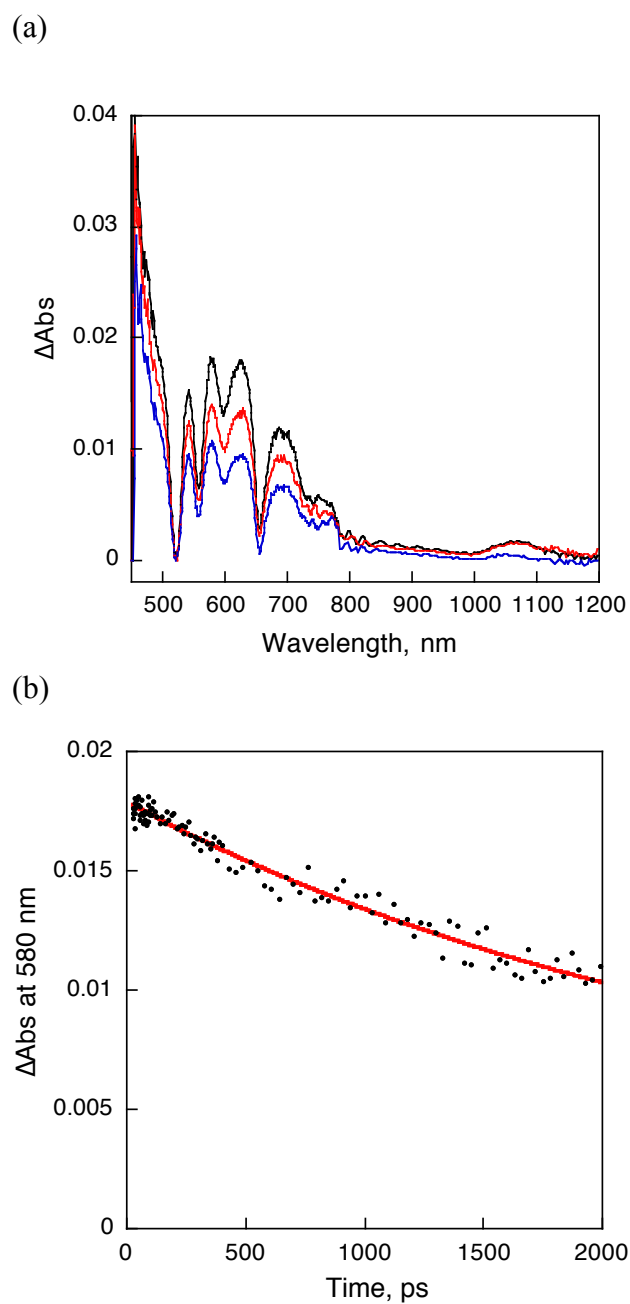
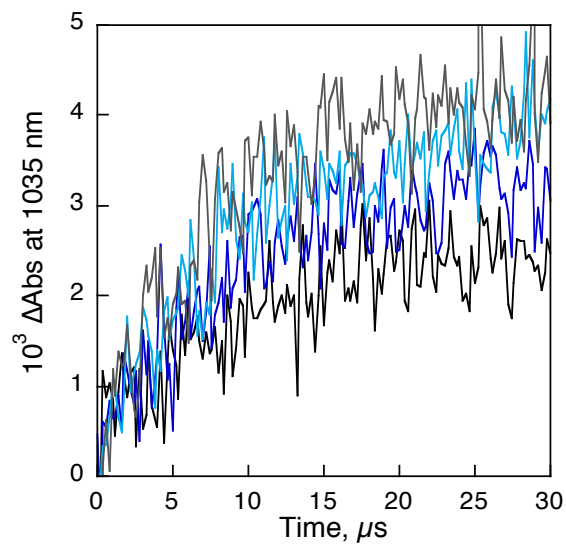


Fig. S12 (a) Transient absorption spectra of $\text{P}(\text{H}_2\text{P})_2$ (5.0×10^{-6} M) with $\text{Li}^+\text{@C}_{60}$ (2.0×10^{-5} M) in deaerated PhCN observed after femtosecond laser flash excitation. Excitation wavelength: 425 nm. (b) Decay time profile at 580 nm with a three-exponential decay curve fitting.

(a)



(b)

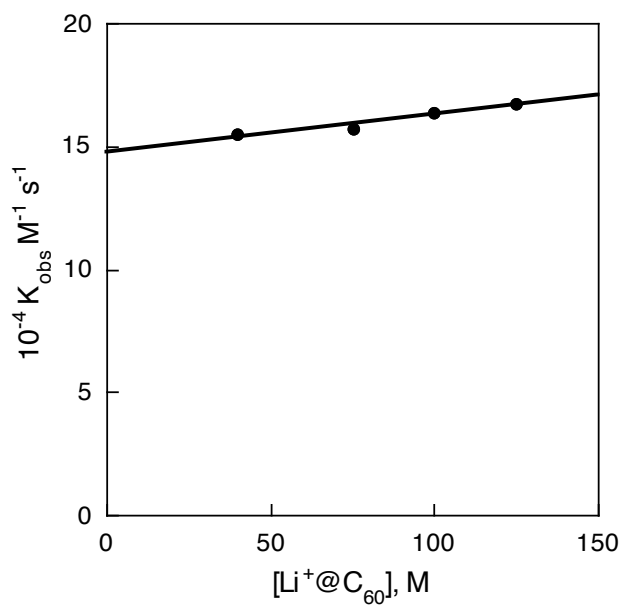


Fig. S13 Rise time profile at 1035 nm with the different laser pulse intensities (2 - 5 mJ pulse⁻¹) in the transient absorption spectral measurements of P(H₂P)₈ (2.6×10^{-6} M) with Li⁺@C₆₀ (40, 75, 100, 130 μM) in deaerated PhCN observed after nanosecond laser flash excitation at 532 nm. (b) Plot of k_{obs} vs. $[\text{Li}^+@C_{60}]$.

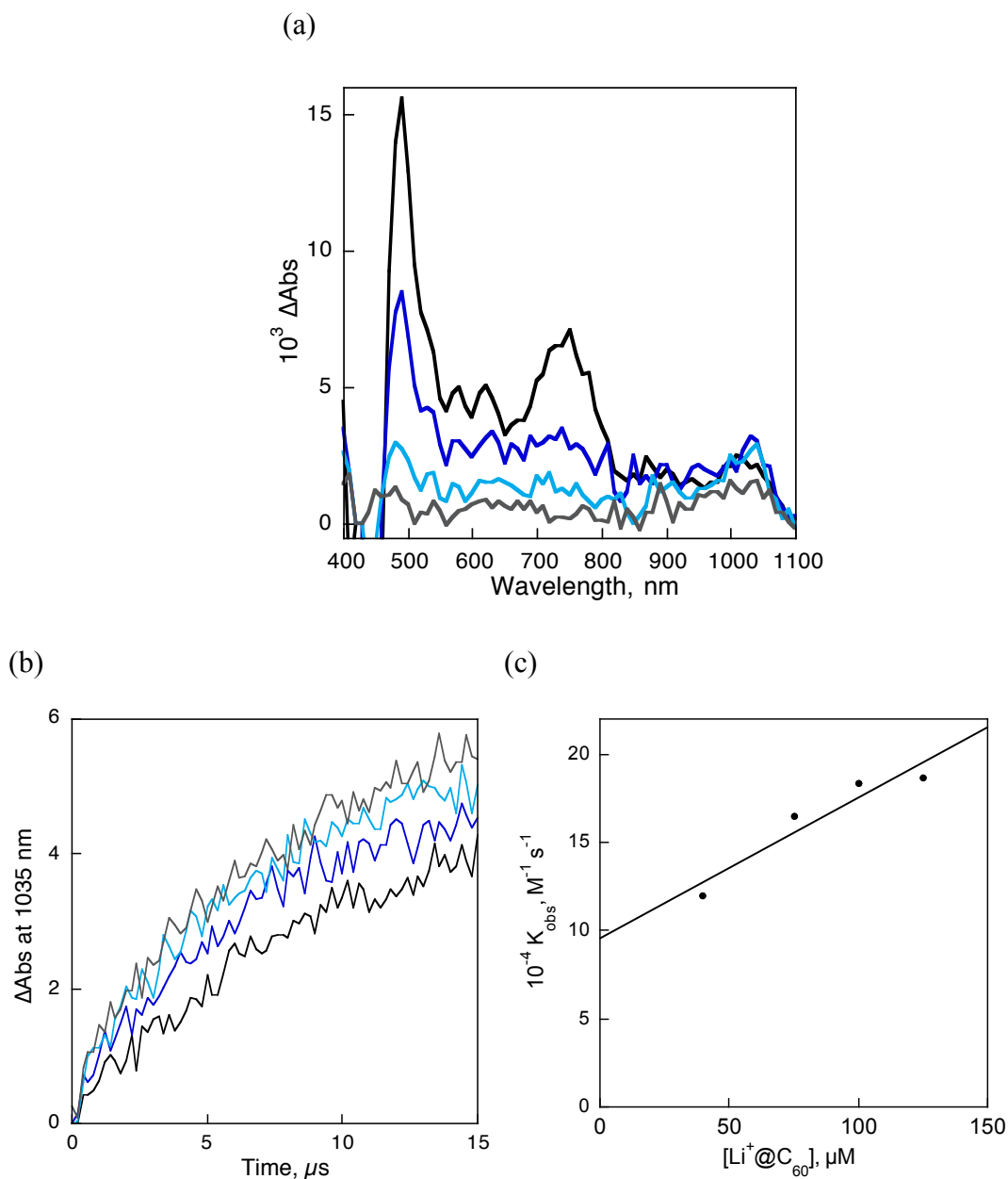


Fig. S14 (a) Transient absorption spectra of $P(H_2P)_4$ ($2.6 \times 10^{-6} M$) with $Li^+@C_{60}$ ($4.0 \times 10^{-5} M$) in deaerated PhCN observed after nanosecond laser flash excitation taken at 8 (black), 32 (blue) and 96 (sky blue) and 200 μs (gray). Excitation wavelength: 532 nm. (b) Rise time profiles at 1035 nm with the different concentration of $Li^+@C_{60}$ (40, 75, 100 and 130 μM). (c) Plot of k_{obs} vs. $[Li^+@C_{60}]$.

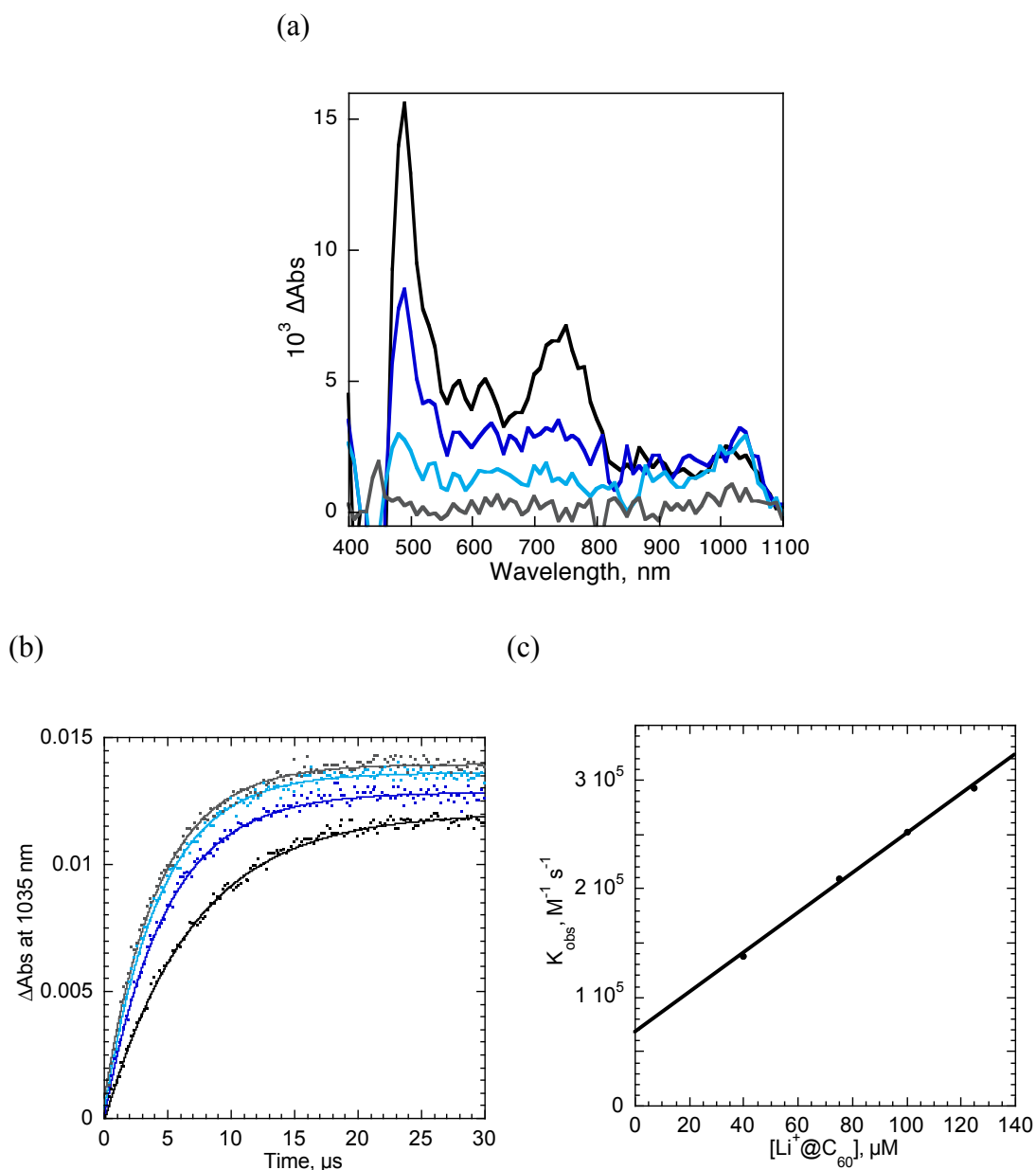


Fig. S15 (a) Transient absorption spectra of $\text{P}(\text{H}_2\text{P})_2$ ($2.6 \times 10^{-6} \text{ M}$) with $\text{Li}^+\text{@C}_{60}$ ($4.0 \times 10^{-5} \text{ M}$) in deaerated PhCN observed after nanosecond laser flash excitation taken at 8 (black), 32 (blue) and 96 (sky blue) and 200 μs (gray). Excitation wavelength: 532 nm. Rise time profiles at 1035 nm with the different concentration of $\text{Li}^+\text{@C}_{60}$ (40, 75, 100 and 130 μM). (c) Plot of k_{obs} vs. $[\text{Li}^+\text{@C}_{60}]$.

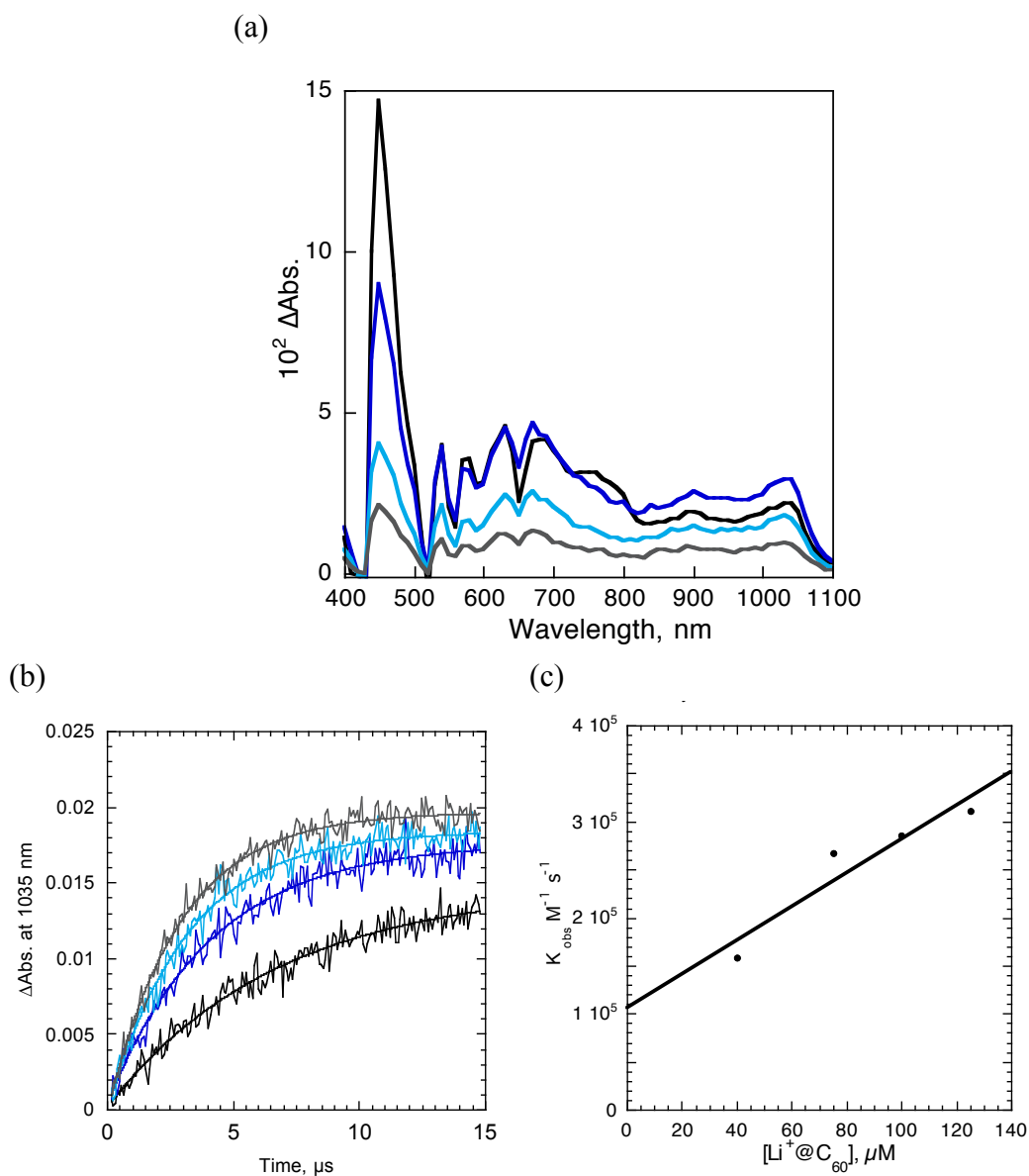


Fig. S16 (a) Transient absorption spectra of $\text{P}(\text{H}_2\text{P})_1$ ($2.6 \times 10^{-6} \text{ M}$) with $\text{Li}^+@\text{C}_{60}$ ($4.0 \times 10^{-5} \text{ M}$) in deaerated PhCN observed after nanosecond laser flash excitation taken at 8 (black), 32 (blue) and 96 (sky blue) and 200 μs (gray). Excitation wavelength: 532 nm. (b) Rise time profiles at 1035 nm with the different concentration of $\text{Li}^+@\text{C}_{60}$ (40, 75, 100 and 130 μM). (c) Plot of k_{obs} vs. $[\text{Li}^+@\text{C}_{60}]$.

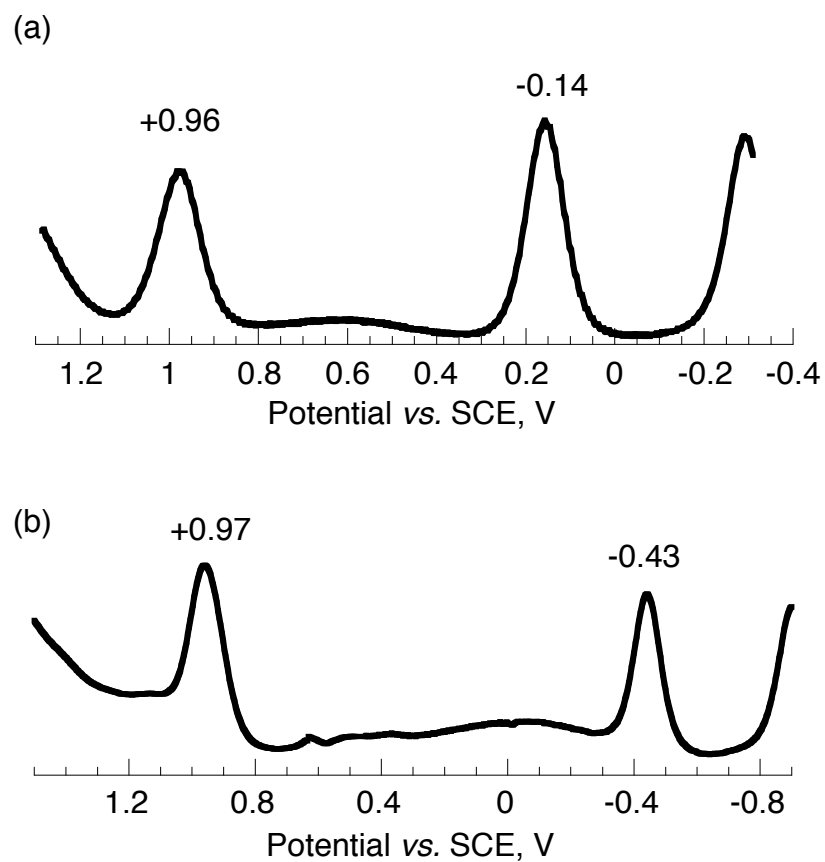


Fig. S17 Differential pulse voltammograms of (a) $P(H_2P)_8$ (0.25 mM) with $Li^+@C_{60}PF_6^-$ (0.20 mM) and (b) $P(H_2P)_8$ (0.25 mM) with C_{60} (0.20 mM) in deaerated PhCN containing $TBAPF_6$ (0.1 M). Scan rate: 4 mV s^{-1} .